Unitarity and the QCD-improved dipole picture

M. McDermott[1], L. Frankfurt[2], V. Guzey[3,4], M. Strikman[3]

[1] Department of Physics and Astronomy, University of Manchester, Manchester M13 9PL, UK
[2] Nuclear Physics Department, School of Physics and Astronomy, Tel Aviv University, 69978 Tel Aviv, Israel
[3] Department of Physics, Penn State University, University Park, PA 16802-6300, USA
[4] Special Research Centre for the Subatomic Structure of Matter (CSSM), University of Adelaide, 5005, Australia

Abstract. As a consequence of QCD factorization theorems, a wide variety of inclusive and exclusive cross sections may be formulated in terms of a universal colour dipole cross section at small x. It is well known that for small transverse size dipoles this cross section is related to the leading-log gluon density. Using the measured pion-proton cross section as a guide, we suggest a reasonable extrapolation of the dipole cross section to the large transverse size region. We point out that the observed magnitude and small x rise of the gluon density from conventional fits implies that the DGLAP approximation has a restricted region of applicability. We found that 'higher twist' or unitarity corrections are required in, or close to, the HERA kinematic region, even for small 'perturbative' dipoles for scattering at central impact parameters. This means that the usual perturbative leading twist description, for moderate virtualities, $1 < Q^2 < 10 \text{ GeV}^2$, has rather large 'higher twist' corrections at small x. In addition, for these virtualities, we also find sizeable contributions from large non-perturbative dipoles ($b \gtrsim 0.4$ fm) to F_2, and also to F_L. This also leads to deviations from the standard leading twist DGLAP results, at small x and moderate Q^2. Our model also describes the low Q^2 data very well without any further tuning. We generalize the Gribov unitarity limit for the structure functions of a hadron target to account for the blackening of the interaction at central impact parameters and to include scattering at peripheral impact parameters which dominate at extremely large energies.

1 Introduction

In the proton rest frame, at small enough $x = Q^2/W^2$ and $Q^2 \gg m_p^2$, Deep Inelastic Scattering of a virtual photon from a proton may be viewed as being factorized into a three stage process: the formation of a state which in general is build of quark, antiquark and gluons from the virtual photon, the scattering of this state off the static proton and the subsequent formation of the hadronic final state. In QCD, the different quark-antiquark-gluon configurations in the photon clearly have different interaction strengths with a target.

For states of very small transverse spatial size, b^2, the dominant scattering state is a quark-antiquark colour dipole state (in this simple case b is the transverse diameter of the dipole). This small dipole has a small scattering probability, which has been calculated in perturbative QCD, and at small x is related to the gluonic colour field associated with the bound state.

The fact that such a dipole cross section appears in a wide variety of hard small x inclusive, exclusive (e.g. heavy vector meson production, DVCS, etc) and diffractive processes is a consequence of the feasibility of separating scales in QCD [1], and may be formulated in terms of a

universal[1] dipole cross section at small x. So far, general, relatively ad hoc, ansätze have been ascribed to this quantity [2,3] and the phenomenological parameters specified by successful fits to structure function data.

States of larger transverse size will in general have much larger cross sections and will contain many constituents. With the increase of the size of the quark-gluon configurations the number of degrees of freedom in the photon wavefunction is also increasing (becoming very large in the non-perturbative QCD regime as a consequence of spontaneously broken chiral symmetry in QCD). Nevertheless, the transverse size of the scattering state seems to be an appropriate parameter for the smooth matching between cross sections in the soft and hard regimes. For convenience we will continue to refer to b^2 as the *dipole* size, and the cross section as the dipole cross section, but these terms should be understood to refer to the transverse size and cross section for more general scattering systems for the case of large systems.

The aim of this paper is to exploit the QCD relationship between the small dipole cross section (DCS) and

---

[1] In practice, the kinematical effect of skewness of the amplitude in exclusive processes leads to a partial, but controlled, breakdown of this universality

the gluon density in the proton to build a realistic ansatz, monotonically increasing in b, for the DCS of all transverse sizes. In the large b region, we match onto the measured pion-proton cross section (at $b_\pi = 0.65$ fm), to which we ascribe a gentle rise with energy. We suggest a smooth interpolation in b for the DCS from small b (where perturbative QCD is valid) up to b_π and a smooth extrapolation for even larger transverse sizes.

Using our ansatz, we then analyze the small x structure functions, calculated in b-space which we denote F_L^b and F_2^b. In this picture, they are given by convolutions in b^2 of the square of the light-cone wavefunction of the virtual photons, of the appropriate polarization state, with the DCS. We observe that for large Q^2, F_L^b reproduces approximately the same result as the standard leading-log perturbative QCD formula. This agreement provides a justification for the relationship between four-momentum scales for the gluon density and transverse dipole sizes which we assume in our ansatz ($Q^2 = 10/b^2$, cf. [4–6]). We then produce values for F_2 using our ansatz and, without any fitting, find reasonable agreement with the HERA data at small x, even for the region of low photon virtuality below the input scale for QCD evolution, $Q^2 < Q_0^2$, where our ansatz may be expected to do less well.

It is straightforward to calculate how much of the non-perturbative region at large b contributes to the structure functions. Since F_2 is mainly governed by the transversely polarized photon, the spin structure of the $\gamma_T^* q\bar{q}$ vertex leads to a considerably broader integral in b than in longitudinal case. We illustrate this well known effect graphically (see Figs. 10,11,12). We find that for relatively high $Q^2 = 4 - 10$ GeV^2 a surprisingly big contribution to the integral (as much as 50%) is coming from this 'dangerous' large b region. While much of this non-perturbative piece is attributable to the input distributions in F_2, the fact that it is also present in F_L could indicate a sizeable 'higher twist' contribution for these virtualities coming from the non-perturbative region. This presents a severe challenge to the use of low, and x-independent, input scales in the conventional parton density fits (e.g. the recent MRST analysis [7] uses input scale $Q_0 = 1.0$ GeV).

We note that the small x rise of the structure function F_2 observed at HERA, which may be translated into a large and steeply-rising gluon density at small x, quickly (after only a few gluon radiations in the ladder) leads to a contradiction with unitarity because the DCS for small dipoles becomes of the same size as the pion-proton cross section (which grows much more slowly with increasing energy). To avoid this problem, it is necessary to tame the small x growth of the perturbative DCS. We suggest a way of doing this which modifies our ansatz for the DCS at small x. For small enough x, this taming appears to be required within the weak coupling limit and hence may be related (albeit indirectly and within a restricted range of x) to the four-gluon to two-gluon calculations of Bartels and collaborators (for a discussion of perturbative higher twist effects in QCD, recent developments and references see [9]).

The unitarity limit for the cross section of a spatially-small colourless wave packet with a hadron target (see Sect. 8 of [4]), and especially the theoretical analysis of the amount of diffraction in the gluon channel predicted by QCD [10], show that the restriction to the leading power of $1/Q^2$ should break down for small enough x, possibly within the kinematics of HERA. Moreover, it follows from the application of Abramovsky-Gribov-Kancheli [11] cutting rules that accounting for the next power in $1/Q^2$ (as in [9]) can lead at most to a 25% reduction of the leading twist result without introducing negative cross sections [4]. Thus, it appears that the decomposition into leading and higher twists becomes ineffective in the kinematical region which can be achieved at the next generation of proton accelerators (LHC) or maybe even at the edge of the kinematics of HERA.

The use of the optical theorem for the scattering of small size wave packets off a hadron target makes it possible to deduce a limit (which is an analog of the Froissart limit for hadron-hadron scattering) for the amplitude in DIS and to calculate the boundary for the applicability of perturbative QCD in small x region [4]. It was found that for $x \approx 10^{-4}$, the boundary is $Q^2 \lesssim 10$ GeV^2. This estimate suggests a significant contribution from higher twist effects in the kinematics of HERA for $x \lesssim 10^{-3}$. A more general aim of this paper is to visualize this problem and to evaluate structure functions of DIS at very small x. We show that many features of the very small x behaviour of structure functions can be understood in terms of the geometry of the spacetime evolution of high energy QCD processes.

In the black limit approximation, Gribov [12] deduced the following formulae for the unitarity limit for structure functions of DIS[2]:

$$F_T = \frac{2\pi r_N^2 Q^2}{12\pi^3} \int_0^{\delta s} \frac{M^2 dM^2}{(M^2 + Q^2)^2} \rho(M^2). \qquad (1)$$

Here r_N is the radius of the nucleon and ρ is the normalized spectrum of produced hadronic masses: $\rho(M^2) = \sigma(e^+e^- \to \text{hadrons})/\sigma(e^+e^- \to \mu^+\mu^-)$. The upper limit on the M^2-integral, which imposes the experimentally-observed sharp diffractive peak: $-t_{min}B_D \approx \frac{(M^2+Q^2)^2 m_N^2}{s^2} \frac{r_N^2}{3} \ll 1$, leads to a generic logarithmic energy dependence (B_D is the usual diffractive slope parameter, m_N is the nucleon mass). Strictly speaking this formula is valid for $M^2 \ll s$, or $\delta \ll 1$, satisfying the condition that the interaction for a hadronic system of mass M is close to the unitarity limit. A similar formulae has been obtained for F_L [12] and for the gluon distribution [10].

It is reasonable to ask if, and if so at which x, the black limit will begin to be approached in Deep Inelastic Scattering of a virtual photon off a proton. In other words,

---

[2] Gribov considered scattering off a heavy nuclei for which the black body limit appears more natural than for a nucleon. However, provided one assumes the black limit, Gribov's arguments, and hence the formulae, will hold. For a recent discussion of the black body limit in QCD for DIS off heavy nuclei see [10,13] and references

at which point does the cross section for the scattering of a small colour dipole with the proton target move away from being transparent (due to colour screening) and start to blacken to its geometrical limit ($\sigma_{tot} = \sigma_{el} + \sigma_{inel} = 2\sigma_{inel} = 2\pi(r_N + b)^2 \approx 40 - 50$ mb)? This question is especially acute for F_L and $\partial F_2/\partial \ln Q^2$ where the interaction of spatially small configurations in the wavefunction of the photon dominate. We aim to address this question in a phenomenological fashion in this paper and to generalize Gribov's unitarity limit to QCD by accounting for QCD phenomena which are neglected within the black body limit (see Sect. 6).

This subject has a rich and long history. For the high energy scattering of a hadron from a nuclear target many configurations in the wave function of the fast hadron contribute and it is convenient to characterize the interaction by a distribution, $P(\sigma)$, of scattering probabilities, σ, of its constituent states instead of by the average value of σ (this useful realization pre-dates QCD, see [14]). The qualitative idea of two-gluon exchange as the mediator was suggested by both Low and Nussinov [15,16]. Low [15] also observed that the dipole cross section should be proportional to the transverse area of the object. Miettenen and Pumplin [17] later suggested that scattering eigenstates should be identified with partonic configurations in the scattering systems, implying that the scattering cross sections of particular states should be related to parton densities in the opposing hadrons. In the modern context, for DIS at small x and for sufficiently small b^2, $\sigma \propto b^2 \alpha_s x g(x, b^2)$ and $P(\sigma)$ follows unambiguously from the QCD factorization theorem for hard exclusive processes [1]. For large b^2, our approach is in many respects similar to the aligned jet model of [18] or QCD-improved aligned jet model of [19] where the cross section of small x processes in the non-perturbative regime is expressed in terms of universal dipole cross section at small x, which is matched to the soft meson-nucleon cross section (the similarity holds despite the difference in the source of $q\bar{q}$ pairs).

The paper is organized as follows. In Sect. 2 we discuss the structure function F_L in b-space, introducing a toy model for the DCS for illustrative purposes. Section 3 sets out our realistic ansatz for the DCS in detail, Sect. 4 compares and contrasts it to other models and ideas in the literature. We make some specific, reasonable choices concerning some of the uncertainties involved in specifying the DCS. These choices are necessary in order to make quantitative statements. However, we have also analyzed the precise form of the DCS in detail numerically and investigated the sensitivity of our results to different choices. This analysis will be presented in a separate paper [20]. However, at this point we merely state that the qualitative statements that we make about unitarity and the influence of large dipoles in F_2 at small x are robust with respect to changes in the details. We discuss this in more detail in Sect. 6, where we also consider the kinematic region in which the Gribov's black limit may be reached for scattering at central impact parameters in DIS for some configurations in the photon wave function. We point out

that certain diffractive processes, for example exclusive photoproduction of J/ψ, may act as useful precursors to the onset of this new QCD regime. We conclude in Sect. 7.

2 Basic Formulae and a toy ansatz for the dipole cross section

In this section we examine the cross section $\sigma_L(x, Q^2)$ in b-space using a very simple toy model for the extrapolation of the DCS to large b. Our aim is to familiarize the reader with the b-space formulation of structure functions. For clarity of presentation we employ a very simple and unphysical ansatz for the DCS at large b. We will improve on this toy ansatz in the next section.

It is convenient to use the impact factor (b-space) representation first introduced by Cheng and Wu in considering high energy processes in QED. In b-space the longitudinal structure function, $F_L(x, Q^2)$, may be written [21, 22] in terms of the DCS convoluted with the light-cone wavefunction of the virtual photon squared:

$$\sigma_L(x, Q^2) = 2 \int_0^{1/2} dz \int d^2b \, \hat{\sigma}(b^2) \, |\psi_{\gamma,L}(z,b)|^2, \quad (2)$$

where

$$|\psi_L(z,b)|^2 = \frac{6}{\pi^2} \alpha_{e.m.} \sum_{q=1}^{n_f} e_q^2 Q^2 z^2 (1-z)^2 K_0^2(\epsilon b), \quad (3)$$

in which $\epsilon^2 = Q^2(z(1-z)) + m_q^2$ and for now we set the light quark mass, m_q to zero.

For small dipoles, the DCS is governed by perturbative QCD [23,24] (for an explicit derivation see [24]):

$$\hat{\sigma}_{pqcd}(b^2, x) = \frac{\pi^2}{3} b^2 \, \alpha_s(\bar{Q}^2) \, x g(x, \bar{Q}^2). \quad (4)$$

We employ a phenomenological scaling ansatz $\bar{Q}^2 = \lambda/b^2$ to relate transverse sizes to four-momentum scales (it is possible to prove that this ansatz is a property of the Fourier transform in the LO and NLO approximations but not beyond). We also implicitly assume that the DCS is independent of light-cone momentum sharing variable z. This is a good approximation for the longitudinal case because the average $z \sim 1/2$ dominate in the integral and due to the $z \to 1 - z$ symmetry of the wave function. For the transverse case the end points give a larger contribution and hence this assumption is less justified.

The relationship of (2,3,4) holds to leading-log accuracy in Q^2 (so, for consistency one is forced to use only LO partons and α_s at one loop) and involves taking the imaginary part of the usual box and crossed box graphs. As such this form corresponds only to the dominant inelastic piece of the DCS. We immediately see a practical problem using eq.(4) in the b-integral of (2). There are always regions in the integral, at large b, where the gluon density is not defined and we need to decide what to do. In particular, for fixed λ, the gluon density is not defined for
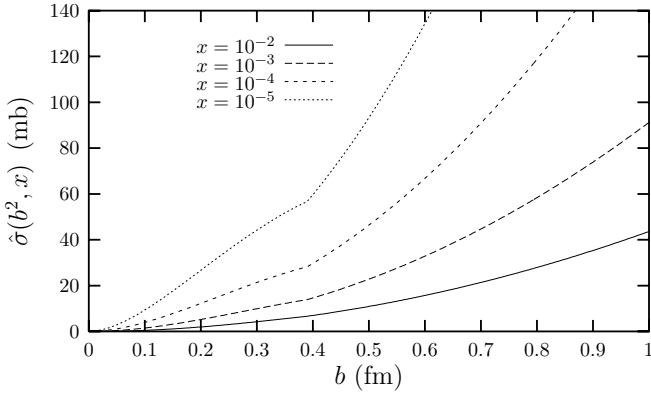
Fig. 1. Dipole cross section in mb for fixed $\lambda = 10$, with the toy model ansatz at large b. For an input scale of $Q_0 = 1.6$ GeV, $b_{Q0} = 0.39$ fm marks the boundary of the perturbative region
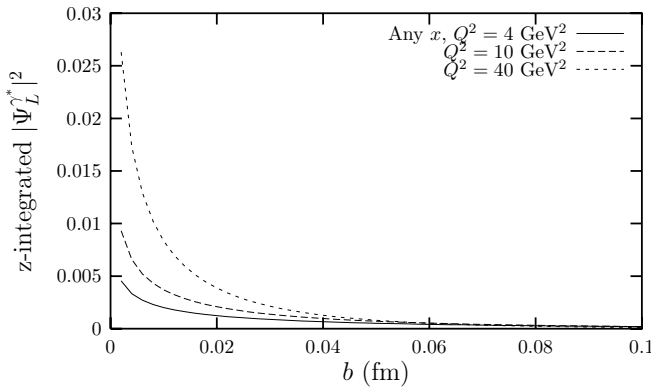
Fig. 2. Longitudinal photon wavefunction squared, integrated over z (in units of fm^{-2}), for $Q^2 = 4, 10, 40$ GeV^2

Fig. 3. Integrand of σ_L, in units of fm, for fixed $\lambda = 10$, $Q^2 = 4$ GeV^2

Fig. 4. Integrand of σ_L, in units of fm, for fixed $\lambda = 10$, $Q^2 = 40$ GeV^2

$b^2 > b_{Q0}^2 = \lambda/Q_0^2$. In the usual treatment this contribution is absorbed into the initial condition of the evolution equations.

To get started we fix $\lambda = 10$ and simply freeze $\alpha_s(\bar{Q}^2)$ $xg(x, \bar{Q}^2)$ at its value at Q_0^2 for $b^2 > b_{Q0}^2$ in (4) (we refer to this as ansatz 1). This means that the DCS retains the canonical b^2-behaviour at large b in (4), and its derivative is discontinuous at $b = b_{Q0}$. Figure 1 shows a plot of the resultant DCS as a function of b for several values of x.

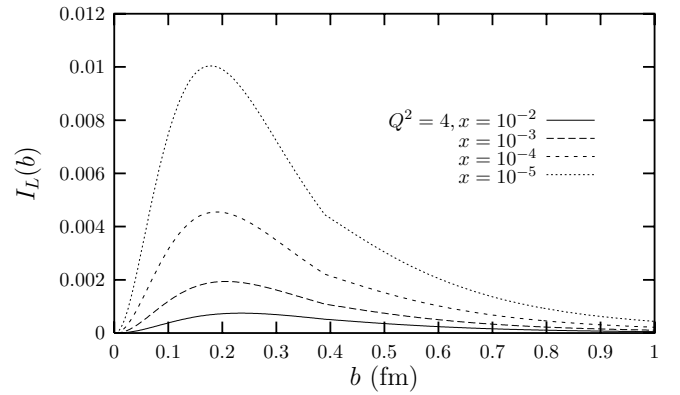We may now examine the dominant regions of the b-integral in eq.(2):

$$\sigma_L(x, Q^2) = \int_0^\infty db\, I_L(b, x, Q^2), \qquad (5)$$

where,

$$I_L(b) = 2\pi b\, \hat{\sigma}(b^2) I_{\gamma, L}, \qquad (6)$$

in which $I_{\gamma, L}$ is the integral of $|\psi_L(z, b)|^2$ over z. Figure 2 shows $I_{\gamma, L}$ as a function of b for three light flavours at fixed values of Q^2, it diverges at small values of b due to the logarithmic divergence of the K_0 Bessel function at small values of its argument.

Figures 3, 4 show the integrand, $I_L(b)$, for two characteristic values of $Q^2 = 4, 40$ GeV^2 using CTEQ4L gluons
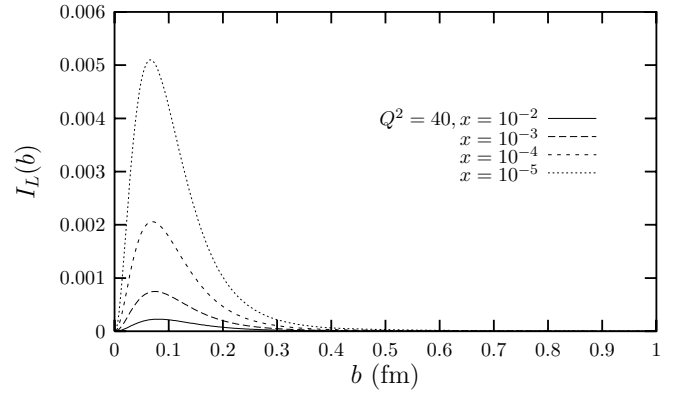
[25]. Note in Fig. 3 one can clearly see that the region above $b_{Q0} \approx \frac{\sqrt{10}}{1.6} * 0.197 \approx 0.4$ fm (where there is a kink due to the freezing of ansatz 1) contributes significantly to the whole integral. In contrast, Fig. 4 shows that for $Q^2 = 40$ GeV^2 (typical effective scale for Υ photoproduction [6]) this region is completely irrelevant. This is due to the fact that the photon piece of the integrand $I_{\gamma, L}$, multiplying the DCS, strongly weights the integrand to progressively smaller b as Q^2 increases (see Fig. 2).

As an example, let us focus on the case when $Q^2 = 40$ GeV^2 and $x = 10^{-3}$. The b-integrand exhibits a strong, slightly asymmetric peak around small $b = b_{\text{peak}} \approx 0.08$ fm, which is slightly skewed to larger b. The relationship $\bar{Q}^2 = \lambda/b^2$, with $\lambda = 10$, implies $Q_{\text{peak}}^2 \approx 60$ GeV^2, and that the typical $b = b_{\text{typ}} \approx 0.1$ fm corresponds to $Q_{\text{typ}}^2 = 40$ GeV^2. Clearly, for $b < b_{\text{typ}}$ the effective scale will be larger than Q^2. The fact that there is very little contribution from the large b-region, for large Q^2, illustrates QCD factorization in b-space: the sharply peaked photon piece of the integrand ensures that only small dipoles contribute significantly in the integral.

We will refer to the structure function $F_L(x, Q^2)$ calculated in b-space as F_L^b. It is related to the defined cross section in the following simple way:
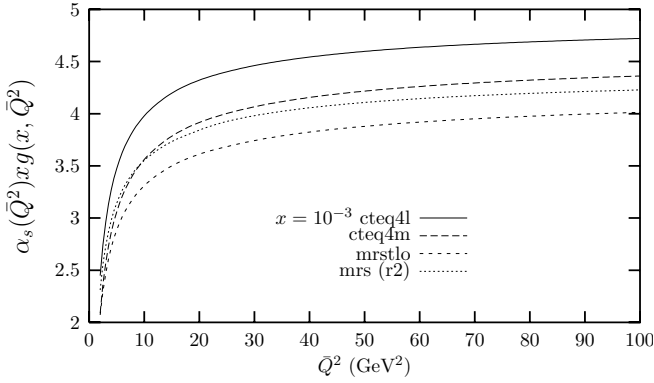
Fig. 5. The function $f(\bar{Q}^2) = \alpha_s x g$ at fixed x for various parton sets

Fig. 6. Integrand of F_L^q versus x'/x for various Q^2 using CTEQ4L gluons

$$F_L(x, Q^2) = F_L^b(x, Q^2, \lambda) = \frac{Q^2}{4\pi^2 \alpha_{e.m.}} \sigma_L(x, Q^2, \lambda) \quad (7)$$

where we have chosen to write the dependence on λ explicitly. Why have we chosen $\lambda = 10$? Lambda should reflect the typical size of contributing dipoles. It may be calculated by defining an average b in the integrand for F_L (in [4–6] a median average of the integral was used). Whatever the precise procedure used for defining the average, a value of $\lambda \approx 10$ comes out for large enough photon virtuality Q^2. Roughly speaking $\lambda = <b>^2 Q^2$, so that when $b = <b>$ the gluon and α_s are sampled at Q^2 in (4) as in the usual leading-log in Q^2 perturbative QCD formula for F_L (see (8) later).

In fact F_L^b has a rather weak dependence on λ for large Q^2, this fact reflects the renormalization group invariance of QCD. We illustrate this in Fig. 5 by plotting $\alpha_s x g$ as a function of its argument at fixed $x = 10^{-3}$ for several LO and NLO parton sets [7,25]. A similar behaviour is observed at other small values of $x < 10^{-2}$. For large $\bar{Q}^2$ it is rather a weak function, and our λ-ansatz translates this into a weak dependence on b. This in turn implies that the canonical $\hat{\sigma}_{pqcd} \propto b^2 \alpha_s(\lambda^2/b^2) x g(x, b^2) \propto b^2$ holds approximately for small enough dipoles. For $x \lesssim 10^{-3}$, $\alpha_s x g$ has positive scaling violations implying an effective behaviour slightly softer than b^2 from QCD at sufficiently small x (the effective $\bar{Q}^2$-power, $\gamma(x, \bar{Q}^2) \lesssim 0.1$ in Fig. 5, for large $\bar{Q}^2 \gtrsim 20$ GeV^2). The peak in b evident in Fig. 4 implies that $\alpha_s x g$ is sampled dominantly only in a small range of $\bar{Q}^2$ in Fig. 5. For small dipoles a reasonable change in λ corresponds to a shift of this dominant region within the fairly flat part of the curve. Hence, as we have checked explicitly, for large Q^2 F_L is insensitive to the precise choice of λ.

However, for smaller scales $\alpha_s x g$ has a much stronger dependence on $\bar{Q}^2$ which tames this linear dependence on b^2 into something much softer. This fact is apparent in the shape of the curves in Fig. 1, for dipole sizes corresponding to the region of $Q_0^2 < \bar{Q}^2 \leq 10$ GeV^2, $\hat{\sigma}_{pqcd}$ deviates considerably from the b^2 behaviour apparent for small ($b \ll b_{Q0}$) and large ($b > b_{Q0}$) dipoles in our toy ansatz. In [20], we investigate this question of interrelation of these scales in more detail. Finally, we note in passing
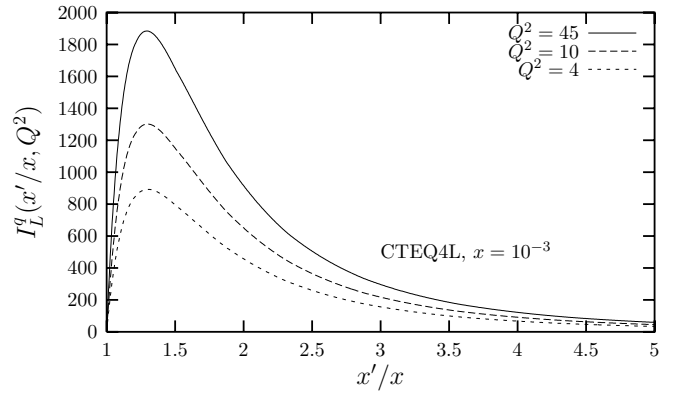
that $\alpha_s x g$, plotted in Fig. 5, has a comparable numerical value and shape for both LO and NLO gluons. Since the dipole cross section is proportional to this quantity for small b, all statements that we make about the size of the DCS using LO gluon densities also hold at NLO.

3 A realistic ansatz for the DCS

At small x, because the gluon density dominates over the quark density, to a good approximation the LO perturbative QCD formula for $F_L(x, Q^2)$ which we denote generically as F_L^q is:

$$F_L(x, Q^2) = \frac{4\alpha_s(Q^2) T_R}{2\pi} \Sigma_{q=1}^{2nf} e_q^2 \int_x^1 dx' x' g\left(x', Q^2\right)$$
$$\times \frac{x^2}{x'^3}\left(1 - \frac{x}{x'}\right). \quad (8)$$

This conventional expression for $F_L(x, Q^2)$ involves an integral over the gluon momentum fraction x', of the proton's momentum p, which feeds into the quark box. In Fig. 6 we plot the integrand of the above formula versus x'/x, at $x = 10^{-3}$, for various Q^2 values. The gluon is sampled at a range of values of $x' > x$ with the integrand, $I_L^q(x'/x)$, peaked around $x'_{peak} \approx 1.3\,x$, and skewed to $x' > x_{peak}$ due to the factor multiplying the rising gluon density. We define an average, $<x>$, to be that x' up to which one must integrate to obtain half of the full integral: it turns out this is always around $x' = <x> \approx 1.75\,x$ for a wide range of external x, Q^2.

Momentum conservation for the fusion of a gluon with a photon, of momentum q, to produce the quark-antiquark pair, of mass $M_{q\bar{q}}^2$, gives

$$(x'p + q)^2 = M_{q\bar{q}}^2 = \frac{k_t^2 + m_q^2}{z(1-z)}$$
$$\geq 4m_q^2 + \frac{k_t^2}{z(1-z)} \propto \frac{1}{b^2}. \quad (9)$$

The inequality in the second line is satisfied for a non-zero quark mass, m_q, when $z = 0.5$. In fact the approximation

$1/(z(1-z)) \approx 4$ holds over a reasonable wide range of z values. So, taking finite quark masses into account implies a minimum value for x' of $x'_{min} = x \, (1 + 4m_q^2/Q^2)$. To account for the important role at large b of confinement and spontaneously broken chiral symmetry we choose constituent quark masses. With this in mind, for our new ansatz we choose to sample the gluon density in (4) at

$$x' = x'_{min} \left(1 + 0.75 \frac{<b>^2}{b^2} \right). \qquad (10)$$

This choice guarantees that for the average b^2, $x' = <x>$, but allows $x'(b^2)$ to vary according to the inverse of the transverse size of the dipoles. Kinematically, a large mass dipole requires a gluon carrying a greater than average momentum fraction to produce it and the ansatz of (10) is designed to reflect this. In contrast, for very large, small mass dipoles $M_{q\bar{q}}^2 \ll Q^2$, and the formula gives $x' \approx x'_{min}$, which is approximately x only for light quarks. The average b is $<b>^2 = \lambda/(Q^2 + 4m_q^2)$, in agreement with the definition of $\lambda = <b>^2 \, Q^2$ in the DIS region, $Q^2 \gg 4m_q^2$, but is infra-red safe in the photoproduction region $Q^2 \lesssim 4m_q^2$.

We also have a constraint on the DCS at large b from the experimental determination of the pion-proton cross section, $\hat{\sigma}_{\pi,N} = 23.78$ mb [26]. The DCS should be close to this at transverse separations which correspond to the diameter of the pion ($d_\pi \approx 0.65$ fm). For rather large $x \approx 10^{-2}$ the magnitude of the DCS at the interface to the non-perturbative region is considerably smaller ($\hat{\sigma}_{pqcd}(x = 10^{-2}, b_{Q0}^2) \approx 6$ mb) than this.

The intermediate region $b_{Q0} < b < b_\pi$ is extremely interesting and very poorly understood, so some modeling is required. It is in this region that strong confinement and effects of spontaneously broken chiral symmetry set in to produce the bound state pion. Clearly the dynamics in this region will include strong colour fields and the creation of light sea pairs from the vacuum. As such, it is no longer reasonable to think of b as corresponding to the transverse size of a dipole. It is better to think of it as corresponding to the typical transverse radius of the complicated non-perturbative system, which in general will contain many constituents.

The minimum requirement of a interpolating function, $\hat{\sigma}_I$ for the DCS is that it matches appropriately at $b = b_{Q0}$ and $b = b_\pi$:

$$\hat{\sigma}_I(x, b^2) = \left[\sigma_{\pi p}(x, b_\pi^2) - \hat{\sigma}_{pqcd}(b_{Q0}^2) \right]$$
$$\times H(b^2) + \hat{\sigma}_{pqcd}(b_{Q0}^2), \qquad (11)$$

with $H(b_{Q0}^2) = 0$ and $H(b_\pi^2) = 1$. On geometrical grounds, we also choose to only consider functions which are monotonically increasing as a function of b. A very simple function which satisfies these requirements is

$$H_1(b^2) = \frac{(b^2 - b_{Q0}^2)}{(b_\pi^2 - b_{Q0}^2)}, \qquad (12)$$

which has a linear growth in b^2, even for $b \approx b_\pi$. To impose a flatter behaviour in this region and a fairly smooth

matching close to $b \approx b_{Q0}$ we choose the following exponential matching

$$H(b^2) = \frac{e}{(e-1)} \left[1 - \exp(-H_1(b^2)) \right], \qquad (13)$$

which retains the linear growth in b^2 close to b_{Q0}.

The pion-proton cross sections is observed to rise slowly as the energy increases. In order to take this into account we impose a slow growth with increasing energy, consistent with a Donnachie-Landshoff soft Pomeron [27], in our boundary condition at $b = b_\pi$:

$$\sigma_{\pi,N}(b_\pi, x) = 23.78 \left(\frac{x_0}{x} \right)^{0.08} \text{mb}, \qquad (14)$$

and choose $x_0 = 0.01$. This behaviour in x is designed to mimic the observed $(W^2/W_0^2)^{0.08}$ behaviour in energy. The precise value of 23.78 mb is taken from the Fermilab data [26] from pion-proton scattering and corresponds to $W_0^2 = 400$ GeV^2.

As x decreases the magnitude of the DCS for small b^2 increases much more rapidly with energy than this soft piece, as a result of the steeply rising gluon density. For leading-log gluons at small enough x, if unchecked, it can even become greater than $\sigma_{\pi,N}(b_\pi, x)$ for perturbative $b < b_{Q0}$. This is clearly nonsensical, some taming of this rapid growth must occur before this can happen. Since the gluon density form of (4) really represents only the inelastic part of the dipole cross section, as it becomes comparable to $\sigma_{\pi,N}$ we need to include the elastic part of the DCS too, which hitherto was implicitly assumed to be negligible. In the limit of very large energy the Froissart bound indicates that the elastic piece should not exceed the inelastic piece. On this basis we really should worry about the applicability of our perturbative QCD formula when the DCS is about 50% of the pion-proton cross section. The absolute upper bound for the inelastic small dipole-nucleon interaction is $8\pi B_{2g}/(1 + \eta^2)$ where $B_{2g} \sim 4 - 5$ GeV^{-2} is the slope of the t-dependence of the two-gluon form factor of the nucleon, as measured in hard exclusive diffractive processes at HERA, and η is the ratio of real and imaginary parts of the scattering amplitude [4,10]. This bound is slightly weaker than the transition point which we assume, but pushing all the way to the absolute limit appears unrealistic.

In our computer code we test $\hat{\sigma}_{pqcd}(x, b^2)$ to see if the equality is reached in the perturbative region $b = b_{crit} < b_{Q0}$, where b_{crit} is defined implicitly by

$$\hat{\sigma}(x, b_{crit}^2) = \frac{\pi^2 b_{crit}^2}{3} \alpha_s(Q_{crit}^2) x' g(x', Q_{crit}^2)$$
$$= \frac{\sigma(x, b_\pi^2)}{2} \qquad (15)$$

with $Q_{crit}^2 = \lambda/b_{crit}^2$ and x' is given by (10). If so, we use a new interpolation in the region $b_{crit} < b < b_\pi$:

$$\hat{\sigma}_I(b^2, x) = \left(\frac{b^2}{b^2 + a^2} \right)^n \sigma_0. \qquad (16)$$

Matching at $b = b_\pi$ sets the value of

$$\sigma_0(x) = \sigma_{\pi,N}(b_\pi, x) \left(\frac{b_\pi^2 + a^2}{b_\pi^2} \right)^n. \qquad (17)$$

The two remaining parameters, a, n, are chosen to provide a fairly smooth matching at $b = b_{crit}$. To achieve this we perform a three parameter fit of exactly the same form as (16) for a given x in the region just below b_{crit}, using MINUIT [28]. We then take the effective power, n_{fit}, from this fit, so that the interpolating ansatz of (16) has approximately the correct power in b^2 at the boundary.

The last remaining free parameter, the scale a, is then specified by the matching at $b = b_{crit}$:

$$a^2 = \frac{b_{crit}^2 \left(1 - (0.5)^{n_{fit}}\right)}{\left(\frac{b_{crit}^2}{b_\pi^2}(0.5)^{n_{fit}} - 1 \right)}. \qquad (18)$$

This ensures a fairly smooth behaviour in b^2 which takes into account the effective behaviour of $\alpha_s(\bar{Q}^2)xg(x, \bar{Q}^2)$ close to b_{crit} as discussed earlier (see Fig. 5).

For very large dipole sizes, $b > b_\pi$, we simply impose a universal residual slow growth, linked to the value at $b = b_\pi$ of the form

$$\hat{\sigma}_I\left(b^2 > b_\pi^2\right) = \sigma\left(b_\pi^2, x\right) \frac{1.5 \, b^2}{(b^2 + b_\pi^2/2)}. \qquad (19)$$

Numerically this very large b region is totally irrelevant for the calculation of DIS structure functions since it is killed by the exponential fall-off of the photon part of the integrand due to the K_0, K_1 Bessel functions (in practice, for moderate Q^2 we integrate up to $b = 1.0$ fm, for smaller $Q^2 < 3.0$ GeV^2 we extend this out to 2.0 fm).

Let us briefly summarize our realistic ansatz. Assuming the universal scaling relation $\lambda = b^2\bar{Q}^2$ restricts the region of applicability of any perturbative QCD dipole formula to transverse sizes smaller than b_{Q0}, which corresponds to the input scale of parton densities in b-space. For small, but not too small x, we use the perturbative QCD formula of (4) with the gluon sampled at x' (see (10)) in the region $0 < b < b_{Q0}$. Between $b_{Q0} \approx 0.4$ fm and $b_\pi = 0.65$ fm we use the interpolating formula of (11), employing the exponential matching of (13). For smaller x, we recognize that $\hat{\sigma}_{pqcd}$ gets too large within the perturbative region $b < b_{Q0}$ at some point, b_{crit}, defined by (15). At this point, we switch from the standard form and use the interpolating form of eqs.(16,17,18), which tames the rapid growth and interpolates in the region $b_{crit} < b < b_\pi$.

In both cases, our ansatz matches onto the pion-proton cross section of (14), at $b = b_\pi = 0.65$ fm, which is allowed a slow Donnachie-Landshoff type energy growth. For $b > b_\pi$ we use the slow increase given in (19). In Fig. 7 we show our new ansatz for the DCS as a function of x. Note, we use the ansatz for both heavy and light flavours. The NA38 collaboration [29] recently suggested $\sigma_{\psi' N} \approx 24 \pm 5$ mb, on the basis of an observed deficit in the number of ψ' decays to dimuons in Sulphur-Uranium collisions relative to well established trends in proton-nucleus collisions. The fact that the large $c\bar{c}(2S)$ bound state has a large interaction cross section with the nucleon in these nuclear collisions, as predicted in [30], is some justification for our flavour
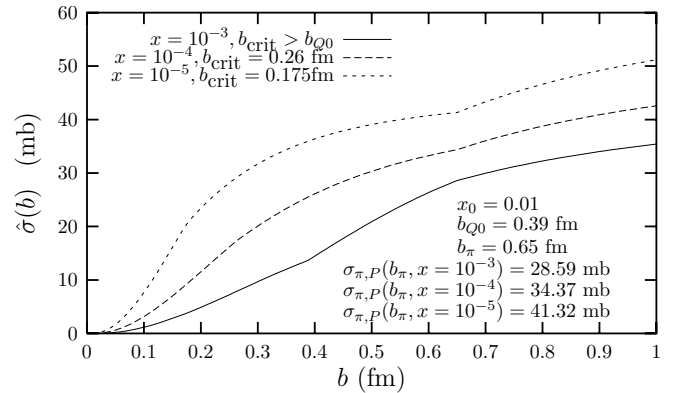
Fig. 7. Dipole cross section in mb for fixed $\lambda = 10$, with the realistic ansatz at large b. For small enough x unitarity corrections are included
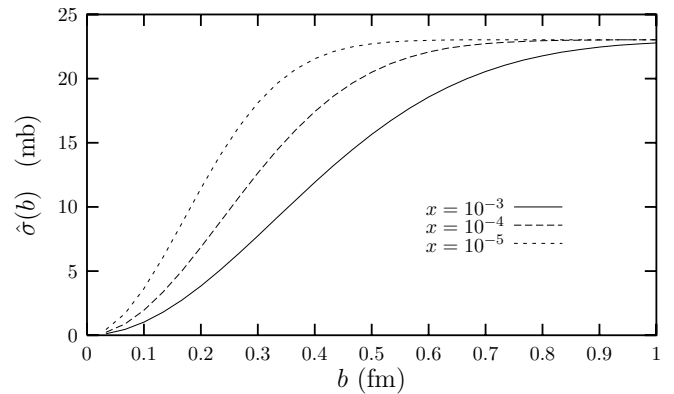
Fig. 8. Dipole cross section in mb for Wusthoff-Golec-Biernat saturation model [2]

blind choice for the DCS in the non-perturbative region ($b \sim 0.6$ fm).

4 Comparison with other models for the dipole cross section

The unitarity correction at small x, discussed above, is clearly beyond the usual DGLAP leading twist analysis and is similar in spirit to the saturating ansatz of Wüsthoff and Golec-Biernat [2]:

$$\hat{\sigma}\left(x, b^2\right) = \sigma_0 \left(1 - \exp\left[-b^2 Q_0^2/4 \left(x/x_0\right)^\lambda\right]\right). \qquad (20)$$

A three parameter fit to the HERA data on DIS with $x < 0.01$, excluding charm and assuming $Q_0 = 1.0$ GeV, produced the following values $\sigma_0 = 23.03$ mb, $x_0 = 0.0003$, $\lambda = 0.288$ and a reasonable χ^2. We are encouraged to note that the "saturation" cross section coming from this fit is considerably below the lowest value of the black limit ($\sigma_{tot}^{black} = 2\pi r_N^2 \approx 40$ mb).

The resultant DCS from (20) is plotted in Fig. 8. A comparison of this figure with our model for σ in Fig. 7 is shown in Fig. 9 which shows the ratio of our σ divided
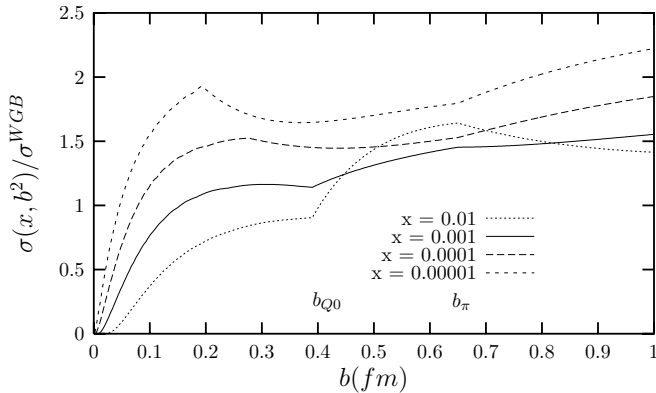
Fig. 9. Ratio of our dipole cross section with the Wusthoff-Golec-Biernat saturation model [2]

by the Wusthoff Golec-Biernat form, σ^{WGB}. It reveals a considerably different b-shape, normalization and energy dependence. Focusing on exclusive processes, which are particularly sensitive to the small b region in which the models differ most, will help to distinguish between them. Having emphasized the contrasts, it is worth pointing out that the two models share some gross features: an approximate b^2 behaviour and strong rise with x at small b, tamed to something much softer at large b. Indeed, the critical point at which we apply our unitarity corrections, b_{crit}, clearly shifts to smaller b as x decreases, as a result of the rising gluon density. This is similar to the critical line of [2].

The form of (20) was clearly chosen with simplicity in mind and is indeed impressively economical in its number of parameters. We recognize this motivation and so do not wish to criticize it too strongly. However, we feel this simple form misses several known crucial features which our ansatz includes (leading to the differences manifest in Fig. 9). Firstly, the small dipole form is known from perturbative QCD (having specified the relationship between b and Q^2, see (4)). The fact that the gluon density may be taken from the global fits allows a careful study of the deviation from a simple b^2 behaviour inherent in (20). As a result the difference between our σ and σ^{WGB} for the perturbative region of $b \leq 0.4$ fm is large and strongly energy dependent (cf. Fig. 9). Using the fitted gluon density also allows the precise behaviour in x to be incorporated more correctly than a single global power implied by (20). Secondly, it is well established experimentally that soft dipole cross section increases slowly with energy. This may be modeled with a small power as in (14) or with a logarithm according to theoretical prejudice. However, (20) has a flat behaviour in energy for large dipoles, leading to a rather large and energy dependent difference for large b. Thirdly, as discussed above, the region where unitarity has to be included is known from the requirement of smallness of the elastic cross section as compared to the total cross section.

The eikonal form assumed in [2], i.e. (20), was inspired by an earlier work by Gotsman, Levin and Maor [31] (see also [32]) in which the hard cross section $\sigma^{inel}_{pqcd} \propto \alpha_s xg$

[23] explicitly appears in the eikonal[3]. At the same time the eikonal approximation has problems in accounting for the generic properties of QCD. In particular, the eikonal approximation assumes conservation of bare particles in the wave function of the photon despite the fact that operators of Lorentz boosts do not commute with the operator of the number of bare particles. A related problem is that the eikonal approximation neglects the energy lost by an energetic particle in the inelastic collisions. Hence, the taming of the increase of parton distribution by this method strongly overestimates the energy released in inelastic collisions.

The recent paper of these authors with Naftali [33], appears to be somewhat orthogonal to their earlier works [31,32] in that the problem of σ^{inel}_{pqcd} getting too large is not addressed. They discuss different regions in the mass of the scattering state, in contrast to dipole sizes (cf. (1)). Roughly speaking, large masses correspond to small dipoles (at least for the lowest $q\bar{q}$ Fock state) and are related to the unintegrated gluon density in this hard contribution. The small mass region is modeled using a Regge analysis. As we have discussed in the current paper (see also [34]), they also stressed the interplay of short and long distance physics to all processes at small x. This correspondence between masses and regions in transverse size is known to break down for higher order Fock states due to the possibility of large size and large mass aligned jet type configurations (see e.g. [35]).

An important point of our analysis, which has been stressed elsewhere including in [4,31,32], is that it is the magnitude and increase of the gluon density within the DGLAP approximation as x decreases that leads to conflict with unitarity. However, in contrast to [2,31,32] we predict that structure functions continue to increase significantly with energy above the unitarity limit as a result of important role of peripheral collisions. This is because unitarity only restricts the contribution to structure functions related to the collisions at central impact parameters (see Sect. 6).

Forshaw, Kerley and Shaw [3] propose a general, rather *ad hoc*, ansatz for the DCS, which they stress is modeled as a function of b^2 and W^2 (rather than x), with a soft Pomeron and a hard Pomeron piece:

$$\hat{\sigma}(W^2, b) = a \frac{P_s^2(b)}{1 + P_s^2(b)} (b^2 W^2)^{\lambda_s}$$
$$+ b^2 P_h^2(b) \exp(-\nu_h^2 b)(b^2 W^2)^{\lambda_h}, \quad (21)$$

where $P_s(b)$ and $P_h(b)$ are polynomials in b. They successfully fit this general form to the data. From the point of view of very large dipoles (of the order of a meson size) one may think that the DCS should be a function of W^2 rather than $x = Q^2/W^2$, since it should just depend on the energy of the collision (here there is no hard scale with which to specify an 'x'). However the presence of a finite x

---

[3] However, we remind the reader that if σ^{inel}_{pqcd} is large enough to require eikonalization then σ^{el}_{pqcd} will also be so large that in the black limit one has $\sigma^{tot} = \int d^2\rho(2 - 2\exp(-\sigma^{tot}_{pqcd}T(\rho)/2))$ within the eikonal approximation

imposes off-forward, or skewed, kinematics which cannot be ignored even in the limit of soft interactions. One can see this for example in the Aligned Jet Model where the propagator for a transition from negative mass-squared $(-Q^2)$ to positive mass-squared of the $q\bar{q}$ pair is present for DIS. Hence, in order to achieve the observed approximate Bjorken scaling of F_2 it was necessary to model the DCS in (21) as a function of $b^2 W^2$, rather than W^2 alone. It is interesting to note that with our ansatz for the relationship between small dipole sizes and hard four-momentum scales, this reduces to an x'-dependence for small dipoles $(b^2 W^2)^n \to (\lambda W^2/Q^2)^n \propto x^{-n}$. For small dipoles, in our approach, there is an identifiable set of diagrams which contain the fusion of a gluon with the virtual photon, hence the DCS can and must depend on the momentum fraction x' of the incoming gluon. How, and whether, this x−dependence becomes a W^2 dependence for large dipoles, and whether it is possible to define the DCS as a unique function over the whole range in b, are interesting and open questions which deserve further consideration. We also note that the DCS which results from the fit of eq.(21), has the rather unattractive feature at large (fixed) energies that it is not a monotonically increasing function of b, it contains a minimum in the region $b \approx 0.6$ fm for $s = 10^5$ GeV^2 (see Fig. 6,7 of [3]). By design, our ansatz specifically avoids this, for fixed x.

From a radically different point of view, we have arrived at a broadly similar picture to Donnachie and Landshoff's two Pomeron model [36], with the soft Pomeron becoming of increasing less importance as the hardness of the process increases (commonly called 'higher twist'). The approximate scaling observed in $\alpha_s xg$ in Fig. 5 explains why a single power in energy will work fairly well for the hard piece. At the same time there are important differences, in our picture for intermediate b the power is different from either of the Pomeron powers of [36] and description of it by the sum of two powers is only approximate and looks rather artificial from the point of view of the dipole picture. Even more importantly, due to unitarity effects and the important role of peripheral collisions we expect a change of the power at higher energies making it closer to the soft Pomeron case. For example, in exclusive production of J/ψ the logic of our ansatz suggests that the large power observed at HERA will become tamed to a smaller power at even higher energies due to unitarity corrections. In contrast, in the two Pomeron picture of [36] the harder Pomeron would completely dominate at higher energies.

5 Testing our ansatz: comparison with structure functions

In Sect. 2, we argued that for very large Q^2 the integrand in σ_L is strongly peaked in the perturbative region and has very little influence from non-perturbative effects in the large b region. If this is really the case, and our ansatz is reasonable, we should be able to reproduce values for the structure function $F_L(x, Q^2)$ which are in close agreement

Table 1. A comparison of the b-space formula, F_L^b, using our ansatz for the DCS, with the standard perturbative QCD result, F_L^q, for $F_L^{n_f=3}(x, Q^2)$ as a function of x for $Q^2 = 4, 10, 45$ GeV^2. We used CTEQ4L gluons

| x CTEQ4L	F_L^q	F_L^b	% diff. $= 100 \times$ $(F_L^q - F_L^b)/F_L^q$	$R_L(\%)$
$Q^2 = 45$				
10^{-2}	0.0638	0.0716	-12.3	5.1
10^{-3}	0.224	0.225	-0.3	2.4
10^{-4}	0.620	0.594	4.1	1.3
10^{-5}	1.53	1.40	8.2	0.7
$Q^2 = 10$				
10^{-2}	0.0704	0.0750	-6.53	26.2
10^{-3}	0.204	0.187	8.46	15.2
10^{-4}	0.493	0.427	13.4	9.87
10^{-5}	1.10	0.869	21.1	6.38
$Q^2 = 4$				
10^{-2}	0.0714	0.0759	-6.32	54.3
10^{-3}	0.174	0.153	12.0	37.5
10^{-4}	0.378	0.307	18.6	26.9
10^{-5}	0.787	0.558	29.1	19.4

with the standard leading-log perturbative QCD formula of (8). As Q^2 decreases towards the input scale Q_0^2 we might expect the two formula to deviate since the large b region is implicitly excluded from the leading twist perturbative QCD formula. For consistency we use the same parton set in each and to avoid the complexities of treating massive charm, in this theoretical cross check, we run with only three light flavours of quarks (we also set the three light quark masses to zero).

Table 1 reveals the excellent agreement of the b-space formula with perturbative QCD at large Q^2 and also displays the deviation of the two formula for low Q^2. Also shown, in the last column is the percentage, $R_L(\%)$, of the b-integral coming from the non-perturbative region above $b > b_{Q0}$. As expected this decreases with increasing Q^2. We used CTEQ4L parton distributions which have an input scale of $Q_0^2 = 2.56$ GeV^2.

Having found reasonable agreement with this theoretical cross check of our ansatz for the DCS, we proceed to calculate its predictions for $F_2(x, Q^2)$, which we denote, F_2^b. In order to calculate this we need to know the wavefunction squared for transverse photons:

$$|\psi_T(z, b)|^2 = \frac{3}{2\pi^2}\alpha_{e.m.} \sum_{q=1}^{n_f} e_q^2 \left[\left(z^2 + (1-z)^2\right)\epsilon^2 K_1^2(\epsilon b)\right.$$
$$\left. + m_q^2 K_0^2(\epsilon b)\right], \tag{22}$$

where $\epsilon^2 = Q^2(z(1-z)) + m_q^2$. From now on we will use $m_q = 300$ MeV, for u, d, s and $m_c = 1.5$ GeV, for both the longitudinal and transversely polarized photon wavefunctions. The small light quark constituent mass only affects
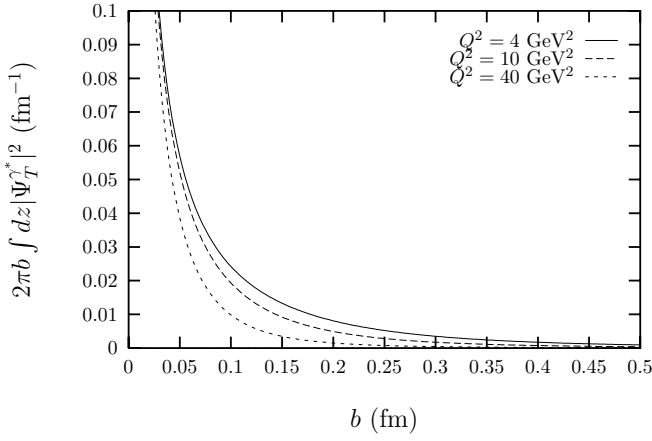
Fig. 10. The weight given to dipole cross section by the transversely polarized photon as a function of transverse size

Fig. 11. The weight given to dipole cross section by the longitudinally polarized photon as a function of transverse size

the structure function seriously in the case of very small $Q^2 < Q_0^2$. It acts as a regulator for the divergence of the Bessel function in the photoproduction limit $Q^2 \to 0$.

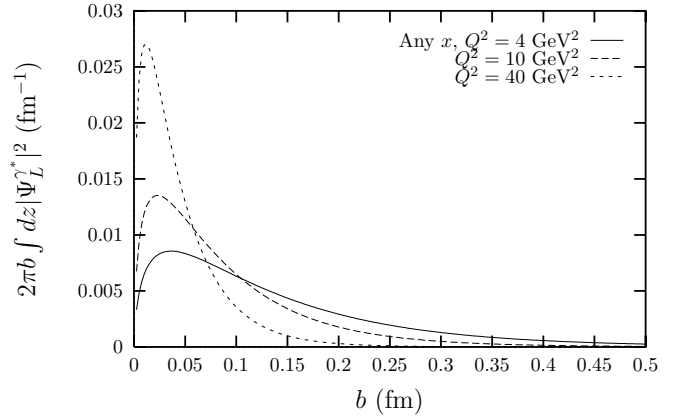We are interested in how $|\psi_T|^2$, integrated over z, weights the dipole cross section in

$$\sigma_T(x, Q^2) = 2\pi\, 2 \int_0^{1/2} dz \int_0^\infty b\, db\, \hat\sigma(b^2)\, |\psi_{\gamma,T}(z,b)|^2$$

$$= \int_0^\infty db\, I_T(b, x, Q^2)\,, \tag{23}$$

where $I_T(b) = 2\pi b\, \hat\sigma\, I_{\gamma,T}$ and

$$I_{\gamma,T}(b) = 2 \int_0^{1/2} dz\, \frac{3\alpha_{e.m} \sum_{q=1}^{n_f} e_q^2}{2\pi^2} \left[(z^2 + (1-z)^2) \right.$$
$$\left. \times \epsilon^2 K_1^2(\epsilon b) + m_q^2 K_0^2(\epsilon b) \right]\,. \tag{24}$$

This integrand, multiplied by the Jacobian factor $2\pi b$, is shown in Fig. 10 as a function of b for three light flavours. At small b, $K_1(a) \propto 1/a$ so $I_{\gamma,T}$ is approximately independent of Q^2 and the residual $1/b^2$, apparent in Fig. 10 cancels the b^2 in (4). As a result, in the perturbative region the transverse cross section, which dominates F_2, is particularly sensitive to the effective behaviour of $\alpha_s x g$ in b. For comparison, Fig. 11 shows $2\pi b\, I_{\gamma,L}$. In contrast, in the longitudinal case $K_0(a) \propto -\ln(a)$ at small a, leaving almost the full power of Q^2 evident in (3), and effects the approximate b^2-behaviour of $\hat\sigma$ very little.

In order to make a comparison of the relative weight that the transverse photon gives to the DCS, we plot the ratio of $I_{\gamma,T}$ and $I_{\gamma,L}$ in Fig. 12. This plot clearly shows that the transverse photon provides support over a much broader range in b, i.e. both at smaller and larger b, than the longitudinal photon. This is especially true at high Q^2 and leads to a very broadly peaked integrand I_T. The peak corresponds approximately to Q^2 and smaller dipoles $b < b_{peak}$ strictly speaking lie outside of the usual leading-log approximation (which result from logarithmic integrations in the perturbative QCD ladder in k_t up to Q^2; the variable b is conjugate to the k_t in the upper quark loop of the ladder in this formulation).
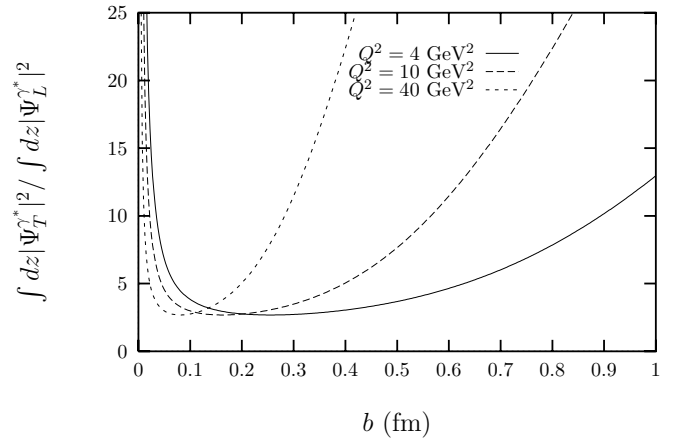

Fig. 12. The ratio of weights, transverse divided by longitudinal, given to the dipole cross section for the two different photon polarizations. Three light flavours are included

The fact that the transverse photon wavefunction squared is so broad in b-space reflects Gribov's paradox (or Bjorken's aligned jet model). At large Q^2 the large dipoles are being produced by asymmetric splittings ($z \ll 1$). While such splittings are unlikely, the large dipoles they produce interact with a large hadronic cross section. The detailed link between large dipoles and asymmetric splittings, and the possibility of a z-dependence in $\hat\sigma$, requires further study. Figures 13, 14 compare the resultant integrands for the transverse and longitudinal photons for large ($Q^2 = 40$ GeV^2) and moderate ($Q^2 = 4$ GeV^2) values of the photon virtuality, respectively. For the latter case, one can clearly seen the unitarity corrections starting to affect the integrands at the smallest values of x. The relative contributions of perturbative and non-perturbative regions are very clear from these figures.

To calculate $F_2^{b(n_f=4)}$ we use

$$F_2(x, Q^2) = F_T + F_L = \frac{Q^2}{4\pi^2 \alpha_{e.m}} (\sigma_T + \sigma_L) \tag{25}$$
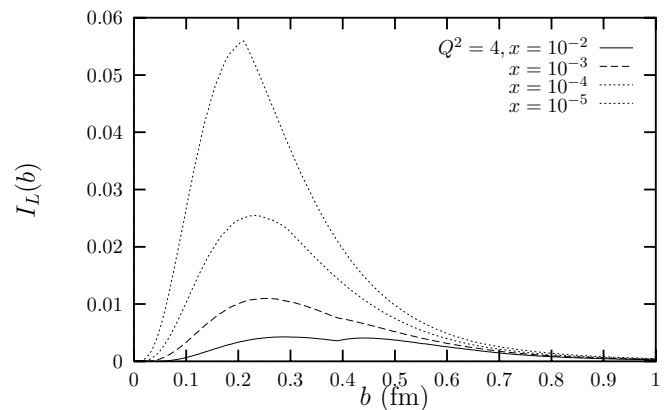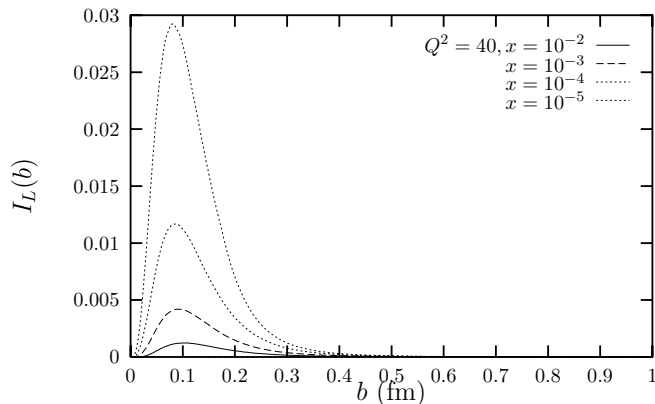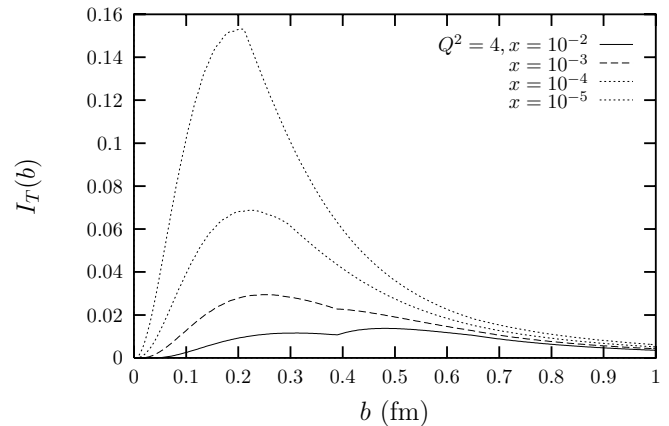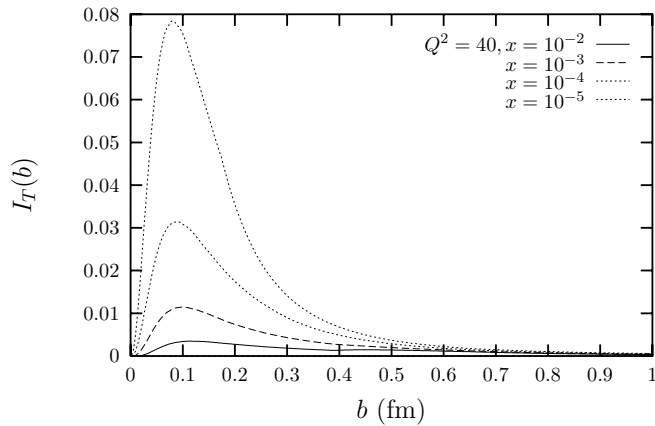
Fig. 13. Integrands in b-space (units mb fm^{-1}) for $Q^2 = 40$ GeV^2

Fig. 14. Integrands in b-space (units mb fm^{-1}) for $Q^2 = 4$ GeV^2

with σ_T defined precisely analogously to σ_L. We also attempt to include threshold effects, albeit in a rather crude way, by imposing that the momentum fraction of the gluon must be sufficient to generate the charm quark pair, using a theta function $\Theta(x' - (Q^2 + M_{cc}^2)/W^2)$. This condition is included in our ansatz of (10) and ensures that $x' > x'_{min} = x\,(1 + 4m_c^2/Q^2)$ for any value of b. This procedure leads to approximately the correct ratio of charm in F_2.

In Fig. 15 we compare our results (solid curves) with the 1994 HERA data [37], [38] for the larger $Q^2 > Q_0^2 = 2.56$ GeV^2 data. Our physical ansatz is in reasonable agreement with the data at small x for moderate values of Q^2. This gives us faith in some of the choices we made in specifying our ansatz for the dipole cross section. Recall that no fitting or minimization procedure has been applied to tune the available parameters to give an excellent fit, although of course it would be possible to do so.

In addition, in Fig. 16 for completeness we show an explicit comparison of our model with the lower $Q^2 < Q_0^2$ ZEUS BPC [39,40] and a selection of the ZEUS SVX [41] data. We could equally have chosen to compare to the low Q^2 H1 data from 1995 [42], which is binned differently in Q^2. It is interesting to note that our model does a reasonably good job in this low virtuality region too, which is most sensitive to our ansatz for the DCS at large b. Again recall that no fitting procedure has been applied.

More recent H1 data, over a wider kinematic range than in [42] was recently presented [43]. Unfortunately the data tables were not publicly available to include in our plots.

Note that in this region of small Q^2 we clearly cannot use DGLAP evolution. At the same time, due to the possibility of separating contributions of small transverse distances in the wave function of the virtual photon with small virtuality we can estimate with rather small uncertainties the short-distance contribution which leads to a fast increase of the cross section with W^2 at fixed Q^2.

6 The onset of the new QCD regime

The small x dipole formulation of high energy processes is attractive in that the contributions from perturbative and non-perturbative regions become very clear. We have extrapolated the perturbative QCD formula for small dipoles into the non-perturbative regime, using the pion-proton cross section as a guide. For very small x it was necessary to tame the growth of the small dipoles to avoid conflict with unitarity.

In our ansatz, small dipoles are governed by the steeply rising gluon density. In principle all high energy processes contain perturbative and non-perturbative contributions, which rise quickly and slowly with increasing energy, re-

F$_2$ (x,Q^2)   **Comparison at intermediate Q^2**
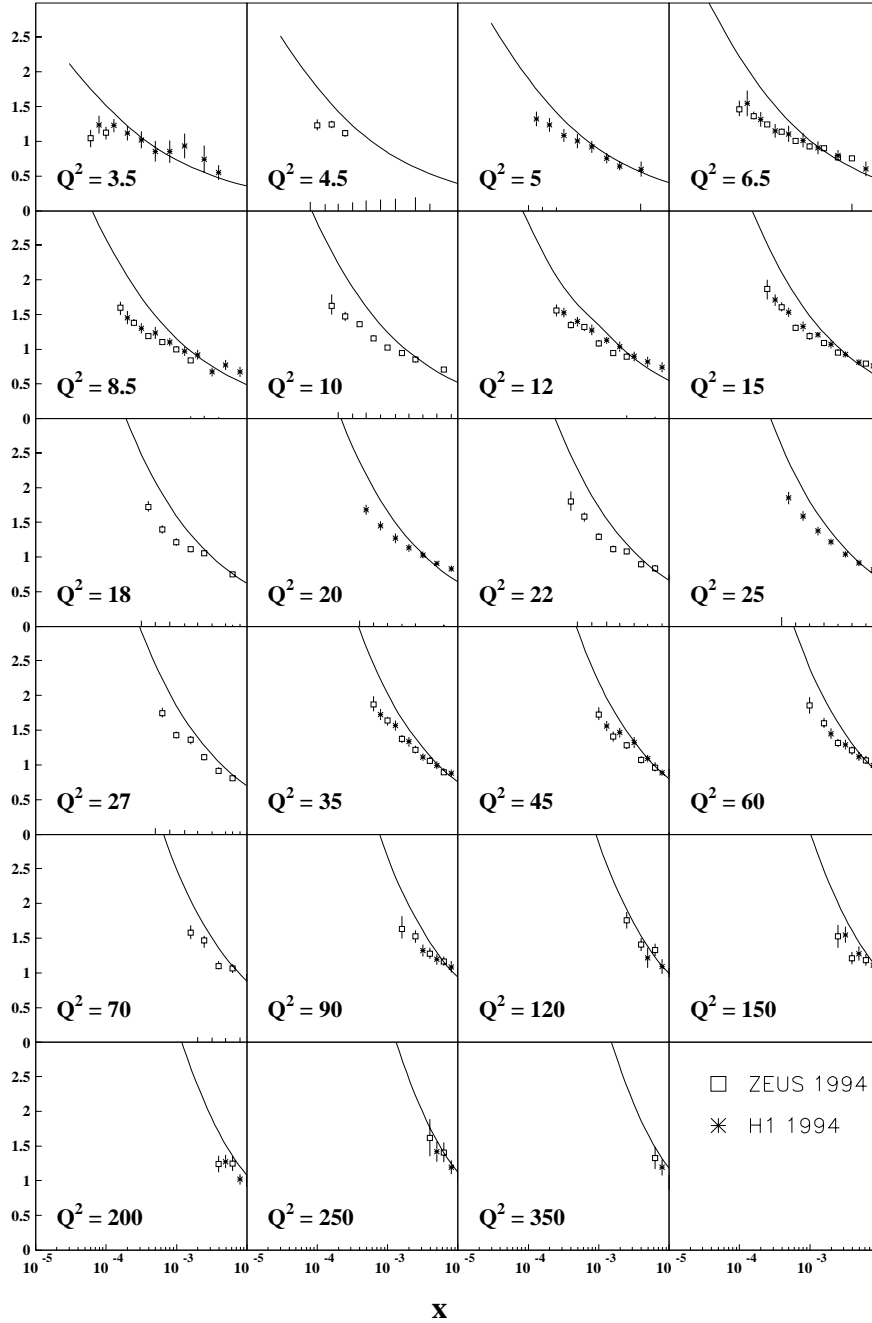
Fig. 15. A comparison of the results with the 1994 data [37], [38], without any fitting procedures

spectively. Having specified the dipole cross section, the light-cone wavefunctions of the external particles pick out a given region in b according to their hardness. A reanalysis of fairly soft exclusive processes, (e.g. electroproduction of ρ-mesons, or DVCS) will be crucial in constraining the large dipole region further.

So, where does this leave the conventional DGLAP analyses of inclusive structure functions which always produce qualitative good fits to the data? In our opinion, the linear nature of the evolution equations mean that the global fits are almost guaranteed to work. When new

data comes out it is always possible to fine tune the functional form of the input, and the many input parameters at the starting scale, to reproduce the slow logarithmic changes in Q^2 in F_2. However, when the resulting quark and gluon densities produce apparent contradictions it is surely time to extend the conventional picture to include other (higher twist) contributions. This is of course very far from straightforward in practice although some interesting attempts have been made [9,44]. A good way to establish experimentally the important role of higher twist effects is to measure diffraction in the gluon channel
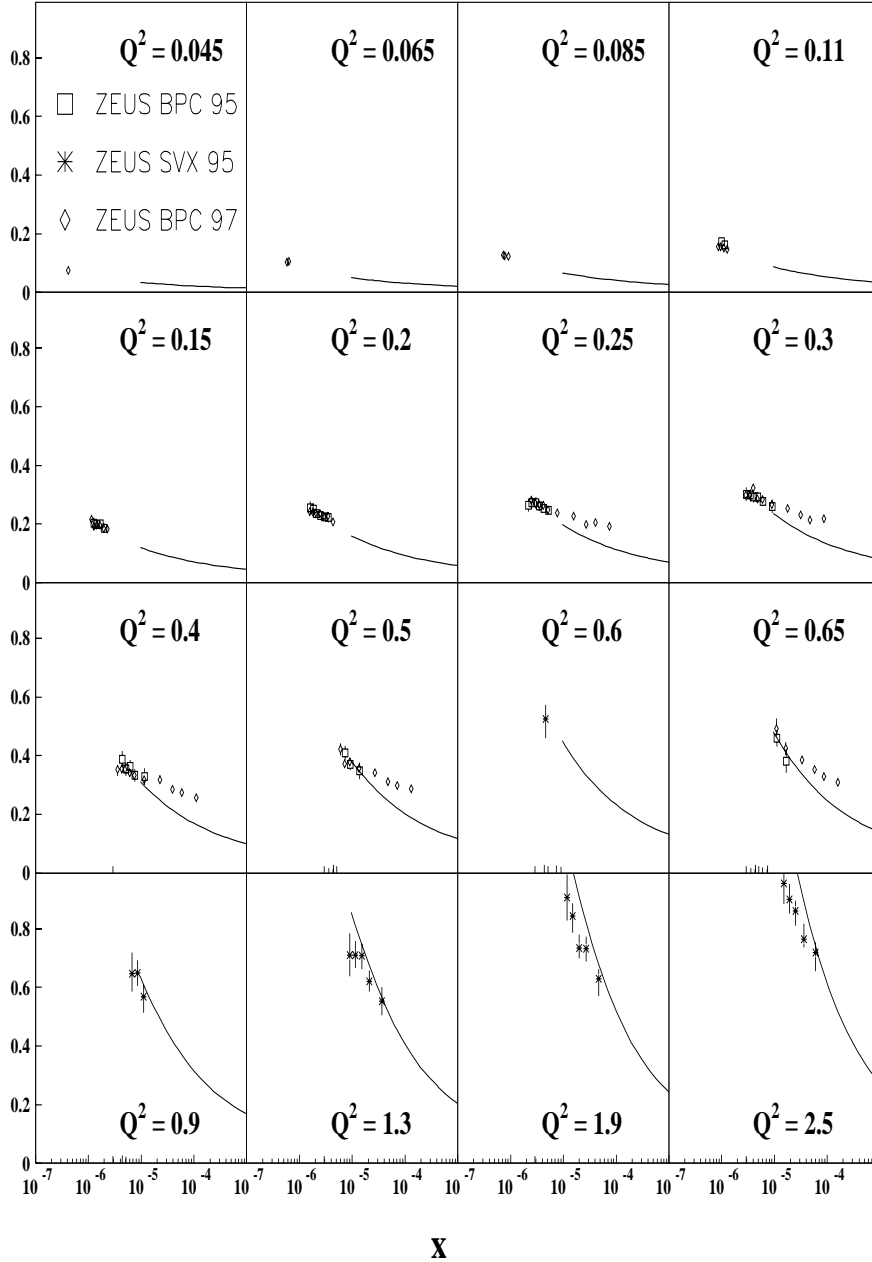
Fig. 16. A comparison of the results with the ZEUS data at low Q^2, without any fitting procedures

and/or diffractive charm and beauty production in DIS (see [10] for discussion).

As well as discussing the transverse size of the scattering system it is also useful, and usual, to discuss the typical *impact parameter*, ρ, of a given configuration on the target (i.e. the conjugate variable to the transverse momentum transfer $q_t : t = -q^2$). Although it is standard to discuss the impact parameter representation of scattering process (see e.g. the textbook by Eden [45]), we have noticed that there is often a confusion between ρ and transverse size b in recent literature. Some useful explicit formulae in this regard are given in the recent paper by Gieseke and Qiao [46]. For particular processes the typical impact parameters are usually expressed in terms of the slope parameter B which specifies the t-dependence (assumed to be exponential).

In hard exclusive diffractive processes in DIS, within the kinematics of HERA, the interaction is typically dominated by scattering at central impact parameters: $\sigma(\rho^2) \propto \exp(-\rho^2/2B)$, where $B \approx 4.5\,\mathrm{GeV}^{-2}$. Thus, very approximately, for these processes $\rho \approx \sqrt{B} \sim 0.6$ fm which is significantly less than the electromagnetic quadratic radius of a nucleon $r_N^{trans.} \approx \sqrt{2r_N^2/3} \approx 0.84$ fm. In contrast, in hadron-hadron collisions peripheral (large ρ) interac-

tions play an important, and perhaps dominant, role. For example, an analysis of elastic proton-proton collisions at Fermilab collider energy range shows that $B \approx 17 \, \text{GeV}^{-2}$ and therefore peripheral $\rho \approx \sqrt{2B} \sim 1.2$ fm are essential in the total cross section. On this basis we can conclude that the spacetime development initiated by a spatially small wave packet of quarks and gluons in DIS is different at the achieved energy ranges from the pattern known from proton-proton collisions, where soft Pomeron physics dominates.

From the analysis of partial waves in high energy ($\sqrt{s} \geq 50$ GeV) elastic $p\bar{p}$ collisions we know that non-perturbative interactions at central impact parameters are close to the black limit and that peripheral collisions play a crucial role. The distinctive feature of DIS, in the kinematics of HERA, which we understand from the above analysis of slopes, is that the scattering at central impact parameters dominates and peripheral scattering, where the interaction is far from black in a wide range of small x, is a correction. The advantage of considering the black regime in DIS is that it is possible to make a complete evaluation of structure functions of a proton, (at least at not too large $Q^2 \approx 1 \, \text{GeV}^2$, i.e. in the regime where nonperturbative QCD physics dominates in the structure functions) because in this limit all configurations interact with the same cross section. Since geometrically, large transverse size dipoles are more likely to correspond to large impact parameters, peripheral collisions should play a much bigger role in σ_T than in σ_L for DIS since the large b plays a much more significant role (cf. Fig. 12).

To demonstrate that our analysis is rather general and almost model independent it is useful to rewrite the equations of the dipole model in a form which accounts for the blackness of interaction for $b^2 > b_0^2$, i.e. to evaluate the black limit of cross section:

$$
\begin{aligned}
&\sigma_{tot}(\gamma_{L,T}^* + p \to X) \\
&= \int dz d^2b \, \hat{\sigma}(z, x, b^2) |\psi_\gamma^{L,T}(z, b, Q^2)|^2 \\
&= 2\pi r_N^2 \int dz d^2b |\psi_\gamma^{L,T}(z, b, Q^2)|^2 \\
&- \int dz d^2b [2\pi r_N^2 - \hat{\sigma}(z, x, b^2)] |\psi_\gamma^{L,T}(z, b, Q)|^2 \theta(b_0^2 - b^2) \\
&+ \int dz d^2b \, \hat{\sigma}_{peripheral}(z, x, b^2) |\psi_\gamma^{L,T}(z, b, Q^2)|^2 . \quad (26)
\end{aligned}
$$

The first term in the last expression is relevant for central collisions and assumes blackness for all dipole sizes[4]: $\hat{\sigma}(z, x, b^2) = 2\pi r_N^2$ (including inelastic and elastic contributions). Alternatively, this black limit of Gribov [12] may be expressed in terms of the structure functions

$$
F_T = \frac{2\pi r_N^2}{12\pi^3} \int_0^{\delta s} \frac{dM^2 \rho(M^2) M^2 Q^2}{(M^2 + Q^2)^2}
$$

---

[4] It is unclear whether the hard amplitude actually achieves the black limit or if the increase of the perturbative QCD amplitude with energy is tamed earlier. Either case leads to the unitarity limit for collisions at central impact parameters

$$
F_L = \frac{2\pi r_N^2}{12\pi^3} \int_0^{\delta s} \frac{dM^2 Q^4 \rho(M^2)}{(M^2 + Q^2)^2} . \quad (27)
$$

As we mentioned in the introduction (cf. (1)) the integral over the mass, M^2, of the intermediate state leads to a logarithm in energy, or equivalently in δ/x:

$$
F_2 = \frac{2\pi r_N^2 Q^2 \rho}{12\pi^3} \ln(\delta/x) . \quad (28)
$$

This estimate is rather close to that obtained within the BFKL approximation ([13] and references therein) which we don't explore in this paper. Based on the equations for the black limit suggested in this paper, which account for the characteristic suppression of the interaction for sufficiently small configurations we may identify δ as the critical scale $x_{crit} = M^2/s$ at which unitarity corrections become necessary for a given s and M^2. An analysis of the black limit in QCD, to be published in a separate paper, shows that for fixed Q^2 δ decreases as x increases, leading to a reduction of the coefficient of $\ln(1/x)$ by a factor of $2-4$ from one for a fixed δ (depending on Q^2). The size of this reduction depends on the rate of increase of $xg(x, Q^2)$ with decreasing x and increasing Q^2.

For Q^2 of a few GeV^2, $x \sim 10^{-5}$ using our estimates of the kinematic range in which unitarity effects may become important we find for δ: $10^{-3} < \delta \sim x_{crit} < 10^{-4}$. This allows us to estimate the numerical values of F_2 for which black limit corrections will be important. For $Q^2 = 1 \, \text{GeV}^2$ $x \approx 10^{-5}$, and taking a reasonable constant $\rho \approx 2.5$, one obtains $F_2^{\text{black}} \approx 1.5 - 3$. This estimate is only a factor of about three bigger than the current HERA measurements.

The second term in (26) corrects for the fact that for small $b < b_0$ this black limit will not yet have been reached, at the x value concerned. This is completely general and does not require a detailed knowledge of the wavefunction of the photon in the large b^2 region. A hypothesis on the blackening of the interaction permits a calculation of the structure functions at very small x which otherwise can not be evaluated within the existing methods of QCD. The second term accounts for the details of QCD phenomena: because of colour screening phenomenon and asymptotic freedom, which are built into the QCD expression for small dipoles (cf. (4)), the Gribov unitarity limit can not be achieved for all configurations in the wave function of a photon. At any particular x, there will exist configurations whose interaction is far from the black limit. So, to evaluate this term it is necessary to make some additional assumptions concerning how the black limit is reached in practice. This introduces some model dependence. For example, one may choose to use our ansatz for $\hat{\sigma}(z, x, b^2)$ with its specific assumption of a smooth interpolation of it to unitarity limit.

The third term of (26) concerns peripheral collisions which will dominate for any initial configuration in the photon wavefunction at extremely small x, due to Gribov diffusion in the parton ladder. The reason for this asymptotic dominance is that for a particular transverse size central collisions will freeze at their black limit, whereas peripheral collisions can continue to grow (albeit slowly)

with energy. For example, for a Donnachie-Landshoff soft Pomeron parameterization [27] they would continue to grow like $\sigma_{\mathrm{peripheral}} \propto (s/s_{\mathrm{black}})^{\epsilon}$.

In this paper we have not tried to elaborate in detail the behaviour of the structure functions in the kinematics where the increase with energy of the perturbative QCD amplitude is slowed down (i.e. where the dipole-nucleon cross section is not far from unitarity limit). In such a kinematic region a dipole of given transverse size b^2 expands with decrease of x to a soft hadronic scale leading to a switch from the perturbative QCD unitarity regime to the soft QCD regime. A distinctive feature of such a scenario will be a fast increase with energy of the slope of the t-dependence of hard exclusive processes.

A similar analysis of the black limit also applies to exclusive process such as diffractive photoproduction and electroproduction of J/ψ. In this case, the black limit applies to the forward scattering amplitude:

$$\frac{A(\gamma^* + P \to J/\psi + P, t = 0)}{is}$$
$$= 2\pi r_N^2 \int dz d^2 b \, \psi_\gamma(z, b^2, Q^2) \, \psi_{J/\psi}(z, b^2). \quad (29)$$

One can then further refine this, at a given x, by breaking the amplitude down into black, not-yet black and peripheral contributions in direct analogy with the decomposition for total cross sections in (26). It follows from this formulae that within the black limit approximation the cross sections of exclusive processes at central impact parameters should not depend on energy. The difference from the structure functions case is because the wavefunction of vector meson suppresses the contribution of small transverse sizes. However, a residual, relatively slow, increase of amplitude with energy is expected due to contributions from peripheral collisions neglected in the above formulae. Since the analysis of quark Fermi motion effects [4,5] revealed that J/ψ photoproduction is dominated by relatively large b, where the unitarity corrections set in early, this is an excellent process in which to search for the onset of the black limit.

Finally, proximity to Gribov's black body limit has important implications for diffraction, which in this limit is equivalent to elastic scattering of quark-gluon configurations in the photon wave function and contributes half of the total cross section (recall that in the black limit $\sigma_{el} = \sigma_{inel} = \sigma_{tot}/2$). Since all component states in the photon have the same cross section non-diagonal transitions in M^2 are absent. We can therefore unfold the M^2-integral in (27) and divide by two to get to the diffractive mass spectrum:

$$\frac{dF_T^{D(2)}(x, Q^2)}{dM^2} = \frac{\pi r_{target}^2}{12\pi^3} \frac{Q^2 M^2 \rho(M^2)}{(M^2 + Q^2)^2} \quad (30)$$

Hence for $M^2 \gg Q^2$ one obtains an expression similar to the triple Pomeron limit with $\alpha_{I\!P}(0) = 1$. The contribution from scattering at peripheral impact parameters, neglected in the black body scenario, would correspond to $\alpha_{I\!P}(0) \geq 1$. The distinctive feature of the final state

is that the average transverse momenta are $\propto M/2$. Let us assume that the black body limit is reached in nature, for example in DIS off heavy nuclei. Since it should be reached at lower energies for large dipoles, the diffractive production of small masses ($M \approx$ few GeV) may serve as an *early signal* for the onset of the Gribov regime. Thus, for a given Q^2 (30) will be valid up to $M^2 \sim Q_{sat}^2$ so that decreasing x expands the region of applicability of this equation.

Note also, as we have argued in [10], that the current diffractive parton density analyses of the HERA diffractive data (see e.g [47]) indicate that gluon induced diffraction at HERA energies maybe already be close to this saturation limit. Unfortunately the lack of measurements of the t-slope of the diffractive amplitude around $Q^2 \sim 4-6$ GeV^2 in gluon induced channels precludes distinguishing between two competing scenarios. Either small sized colour octet dipoles with $\sigma_{eff} \sim$ 30-40 mb dominate (expected $B \sim B_{J/\psi} \approx 4.5$ GeV^{-2}, $\alpha^{'} \ll \alpha_{soft}^{'}, \alpha_{I\!P} - 1 \approx 0.2$) or large colour-triplet dipole with with $\sigma_{eff} \sim$ 50-60 mb dominate (expected $B \sim B_{inclusive} \approx 7$ GeV^{-2}, $\alpha^{'} \sim \alpha_{soft}^{'}, \alpha_{I\!P} - 1 \approx \alpha_{soft}$). The first scenario naturally leads to a behaviour analogous to (30) for the gluon channel for scattering off nuclei. We will consider these phenomena elsewhere.

7 Conclusions

We have proposed a physically motivated ansatz for the dipole cross section (DCS) relevant to a wide range of small x scattering processes. The small dipole cross section is governed by the leading log gluon density at small x. Using this and the measured pion-proton cross section as a guide, we construct an ansatz for it in the non-perturbative region, below the input scale at which the input density for the gluon is defined. At very small values of x, as a result of the large and steeply rising gluon density, the DCS threatens to become larger at small perturbative b than the pion-proton cross section, in conflict with unitarity. To prevent this from happening we tame the rapid growth using a smooth ansatz that ensures a monotonically increasing function of b at fixed x.

The resultant DCS produces values for $F_L(x, Q^2)$ which are in good agreement with those from perturbative QCD in the large Q^2 and the high end of the small x region, where it would be expected to. Our DCS compares reasonably well with all available small x data on F_2 from HERA, without any further tuning of parameters. Interestingly, in the moderate Q^2 region a significant fraction of the cross section appears to be coming from the region of large non-perturbative dipoles. If the perturbative unitarity corrections are neglected our model would continue to grow very steeply in the very small x region. More detailed studies of the choices that we make for the precise form of the ansatz are being carried out and will be reported in a separate paper [20]. Although these clearly affect the results quantitatively to a certain extent, we are confident of the qualitative conclusion of the paper that unitarity

corrections must set in within or near to the HERA kinematic region of small x and moderate Q^2 (we estimate that the $Q^2 < 10$ GeV^2 will be affected at the smallest attainable values of x). This calls into question the use of the low, and x-independent, input scales used in the standard DGLAP fits [7, 25, 48, 49] ($Q_0^2 \approx 0.8 - 2.6$ GeV^2).

In Sect. 6 we generalized Gribov's black limit to the perturbative QCD analysis of DIS to make it compatible with the applicability of the DGLAP approximation at sufficiently large Q^2 but fixed x and with the dominance of peripheral collisions at fixed Q^2 at extremely high energies. We estimate that this black limit is close to the lower edge of the HERA kinematic region in x for $Q^2 = 1$ GeV^2. We suggest that certain diffractive processes may acts as earlier indicators of the onset of this new regime.

References

1. J. C. Collins Phys. Rev. **D57** (1998) 3051; J. C. Collins, L. L. Frankfurt and M. Strikman, Phys. Rev. **D56** (1997) 2982.
2. K. Golec-Biernat, M. Wüsthoff, Phys. Rev. **D59** (1999) 014017; Phys. Rev. **D60** (1999) 114023.
3. J. Forshaw, G. Kerley, G. Shaw, Phys. Rev. **D60** (1999) 074012.
4. L. L. Frankfurt, W. Koepf and M. Strikman, Phys. Rev. **D54** (1996) 3194
5. L. L. Frankfurt, W. Koepf and M. Strikman, Phys. Rev. **D57** (1998) 512.
6. L. Frankfurt, M. McDermott and M. Strikman, **JHEP02** (1999) 002.
7. A. D. Martin, R. G. Roberts, W. J. Stirling and R. S. Thorne, Eur. Phys. J. **C4** (1998) 463; Phys.Lett. **B443** (1998) 301.
8. R. P. Feynman, "Photon-Hadron Interactions", (Benjamin, 1972); Phys. Rev. Lett. **23** (1969) 1415.
9. J. Bartels, C. Bontus, Phys. Rev. **D61** (2000) 034009; J. Bartels, C. Bontus and H. Spiesberger, hep-ph/9908411.
10. L. Frankfurt and M. Strikman, Nucl. Phys. B (Proc. Suppl.) **79** (1999) 671, Proceedings of DIS '99 (DESY Zeuthen, April 1999), eds. J. Blümlein and T Riemann, hep-ph/9907221; Eur. Phys. J. **A5** (1999) 293.
11. V. A. Abramovsky, V. N. Gribov, O. V. Kancheli, Sov. J. Nucl. Physics **18** (1974) 308.
12. V. N. Gribov, Sov. J. Nucl. Phys. **9** (1969), 369; Sov. Phys. JETP **29** (1969) 483; ibid **30** (1970) 709; Zh. Eksp. Teor. Fiz. **57** (1969) 1306.
13. A. H. Mueller, Nucl. Phys. **B558** 285; hep-ph/9911289.
14. M. L. Good and W. D. Walker, Phys. Rev. **120** (1960) 1857; E. L. Feinberg and I. Ya. Pomeranchuk, Suppl. Nuovo Cimento **III**, (1956) 652.
15. F. E. Low, Phys. Rev. **D12** (1975) 163.
16. S. Nussinov, Phys. Rev. Lett. **34** (1975) 1286.
17. H. I. Miettinen and J. Pumplin, Phys. Rev. **D18** (1978) 1696.
18. J. D. Bjorken and J. B. Kogut, Phys. Rev. **D8** (1973) 1341.
19. L. L. Frankfurt and M. Strikman Phys. Rep. **160** (1988) 235.
20. L. Frankfurt, V. Guzey, M. McDermott and M. Strikman, in preparation.
21. H. Cheng and T.T Wu, "Expanding Protons: Scattering at High-Energies" (MIT-Pr.,Cambridge, USA, 1987).
22. N. N. Nikolaev, B. G. Zakharov, Z. Phys. **C49** (1990) 607.
23. L. Frankfurt, G. A. Miller, M. Strikman, Phys. Lett. **B304** (1993) 1; B. Blattel, G. Baym, L. Frankfurt and M. Strikman, Phys. Rev. Lett. **71** (1993) 896.
24. L.Frankfurt, A. Radyushkin and M. Strikman, Phys. Rev. **D55** (1997) 98.
25. H. L. Lai et al, Phys. Rev. **D55** (1997) 1280.
26. A. Carroll et al, Phys. Lett. **B80** (1979) 423.
27. A. Donnachie and P. V. Landshoff, Nucl. Phys. **B191** (1987) 309; Phys. Lett. **B296** (1992) 227.
28. F. James, "MINUIT: function minimization and Error analysis", CERN Program Library Long Writeup **D506**.
29. M.C. Abreu *et al*, NA-38 Collab., **B466** (1999) 408.
30. L. Gerland *et al* Phys. Rev. Lett. **81** (1998) 762.
31. E. Gotsman, E. Levin, U. Maor, Phys. Lett. **B425** (1998) 369
32. E. Gotsman, E. Levin, U. Maor, Eur. Phys. J. **C5** (1998) 303; Nucl. Phys. **B539** (1999) 535;
33. E. Gotsman, E. Levin, U. Maor, E. Naftali, Eur. Phys. J. **C10** (1999) 689.
34. H. Abramowicz, L Frankfurt and M. Strikman, Surveys High Energ. Phys. **11** (1997) 51.
35. W. Buchmueller, M. F. McDermott and A. Hebecker, Nucl. Phys. **B476** (1997) 283, **B500** (1997) 621 (E); A. Hebecker, Acta. Phys. Polon. **B30** (1999) 3777.
36. A. Donnachie and P. V. Landshoff, Phys. Lett. **B437** (1998) 408; J. R. Cudell, A. Donnachie and P. V. Landshoff, Phys. Lett. **B448** (1999) 281.
37. M. Derrick et al, ZEUS Collab., Z. Phys. **C72**, (1996) 399.
38. S. Aid et al, H1 Collab., Nucl. Phys. **B470**, (1996) 3.
39. J. Breitweg et al, ZEUS Collab., Phys. Lett. **B407**, (1997) 432; Z. Phys. **C69**, (1996) 607.
40. J. Breitweg et al, ZEUS Collab., hep-ex/0005018.
41. J. Breitweg et al, ZEUS Collab., Eur. Phys. J. **C7** (1999) 609.
42. C. Adloff et al, H1 Collab., Nucl. Phys. **B497**, (1997) 3.
43. "Measurement of the Proton Structure Function F_2 at very low Q^2 and very low x", M. Klein, H1 Collab., Talk at Lepton-Photon Symposium, Stanford, August 1999.
44. J. Jalilian-Marian, A. Kovner, A. Leonidov and H. Weigert, Phys.Rev. **D59** (1999) 034007; Erratum-ibid, **D59** (1999) 099903 and references therein; L. McLerran and R. Venugopolan, Phys. Rev. **D49** (1994) 2233.
45. R. J. Eden, "High Energy Collisions of Elementary Particles" (Cambridge University Press, 1967).
46. S. Gieseke and C.-F. Qiao, Phys. Rev. **D61** (2000) 074028.
47. L. Alvero, J. C. Collins, J Terron and J. Whitmore, Phys. Rev. **D59** (1999) 074022.
48. M. Glück, E. Reya, A. Vogt, Eur. Phys. J. **C5** (1998) 461.
49. H. L. Lai et al, Eur. Phys. J. **C12** (2000) 375.